Surface characterization study of Ag, AgO, and Ag_2O using x-ray photoelectron spectroscopy and electron energy-loss spectroscopy

Gar B. Hoflund and Zoltan F. Hazos
Department of Chemical Engineering, University of Florida, Gainesville, Florida 32611

Ghaleb N. Salaita
Union Carbide Corporation, Technical Center, 3200 Kanawha Turnpike South Charleston, West Virginia 25303

(Received 22 June 1999)

Electron energy-loss spectra (ELS) have been obtained from polycrystalline Ag metal, AgO powder, and Ag_2O powder using primary electron-beam energies ranging from 100 to 2000 eV. These samples were characterized using x-ray photoelectron spectroscopy (XPS) to determine the compositions and chemical species in their near-surface regions. The ELS spectra obtained from these three materials are significantly different, implying that ELS is a useful technique for distinguishing between Ag metal, AgO, and Ag_2O or analyzing mixtures of these species. Such an analysis is difficult using techniques including XPS or Auger-electron spectroscopy because spectral features of these species are quite similar and closely spaced. The ELS spectral features consist of losses due to the formation of surface and bulk plasmons and interband transitions. An attempt has been made in this study to assign the processes responsible for the ELS features observed in the spectra. This interpretation will be improved as the electronic structures of Ag metal, AgO, and Ag_2O are better understood.

INTRODUCTION

The silver-oxygen system has been studied extensively in the past[1–9] due to its important industrial and technological applications. Among the most important of these is the alumina supported silver-catalyzed epoxidation of ethylene.[10–21] Supported Ag is unique in that it is the only metal that selectively produces ethylene oxide rather than CO_2 and H_2O. A more recent application takes advantage of the high permeability of oxygen through silver membranes[22,23] in order to produce a flux of hyperthermal oxygen atoms[24] by electron-stimulated desorption.[6,25] The study of the silver-oxygen system is complicated by the fact that oxygen is often present in multiple states including atomic, molecular, and subsurface states as reviewed by van Santen and Kuipers.[13] Since the amounts and chemical forms of oxygen present at a Ag surface depend upon the previous history of the sample, it is difficult to study a particular chemical state of oxygen without influence from other states. Another complication in the characterization of the silver-oxygen system is the presence of contaminants. Previous x-ray photoelectron spectroscopy (XPS) studies of AgO and Ag_2O have shown[1,2] that CO_2 present in the air is responsible for the formation of Ag_2CO_3 on these surfaces. The corrosion resistance properties of silver have been attributed in part to the formation of this carbonate layer.[26]

XPS has been used widely to study silver and its oxides because it is capable of providing important chemical-state information about the Ag-O system, although the interpretation of the results is complicated and occasionally controversial. There is general consensus among many studies[1–5,7,8,27,28] that the binding energy (BE) of the Ag $3d$ peaks exhibit a negative shift as the oxidation state is increased. Some earlier studies failed to observe these shifts.[29,30] These shifts are in the range of a few tenths of an eV, which is one of the sources of difficulty in the interpretation of the spectra. Mixtures of Ag metal and oxides are very difficult to study since their Ag $3d$ peaks are so closely spaced. The Ag *MNN* Auger peaks exhibit a somewhat greater shift than the Ag $3d$ peaks during the oxidation of silver, but there is not general agreement in the literature regarding the magnitude of these shifts. Valence-band XPS (VBXPS) often is a useful technique for examining systems that exhibit subtle changes in the XPS core-level spectral features. Generally, more effort will be required to understand the VBXPS data obtained from the silver-oxygen system,[1–5,28,31] but these features also seem rather similar.

Clearly, the study of the Ag-O system is complicated and the analyses of the data obtained from these systems are not straightforward. The purpose of this investigation is to use electron energy-loss spectroscopy (ELS) and XPS to characterize Ag, AgO, and Ag_2O reference samples. XPS provides both compositional and chemical-state information, which is useful in understanding the ELS data. The goal of this research is to develop ELS as a method for distinguishing between different Ag-containing materials including Ag metal, Ag_2O, AgO, Ag_2CO_3, $Ag(NO_3)$, and others. Apparently, ELS data have not been published for Ag_2O and AgO so this present study will serve as a basis for future developments in this area. Attempts are made below to assign the complex spectral features. These results also provide a powerful means of studying Ag chemistry such as the thermal decomposition of Ag_2CO_3.[32,33]

A similar approach has been successful in distinguishing between various tin oxides and metal. This too has proven very difficult using XPS because the Sn $3d_{5/2}$ peaks differ by only 0.2–0.5 eV between SnO and SnO_2.[34–37] Powell[38] first showed that ELS data obtained from SnO and SnO_2 are dis-

tinctively different, making ELS the best surface technique for distinguishing between SnO and SnO_2. VBXPS spectra do exhibit some subtle differences between SnO and SnO_2,[39–42] but it is insensitive[43] to a metastable transitional Sn oxide readily observed[35,40,44,45] by ELS and believed to be Sn_3O_4,[46,47] which is always present at Sn oxide surfaces.

ELS has other advantages over XPS as well. Since an electron beam is used as the primary excitation source, small-spot ELS can be performed with a spatial resolution as low as 10 nm using commercially available scanning Auger microscopy (SAM) systems. By restoring, high-resolution spatial chemical-state distributions can be obtained, i.e., using scanning ELS (SELS). The depth sensitivity can also be varied easily using ELS by varying either the primary-beam energy[40] or the incidence and collection angles.[48] It should be possible to obtain three-dimensional, chemical-state information by performing SELS at different primary-beam energies. Furthermore, the ELS signal strength can be varied over a large range since an electron source with a broad dynamic range provides the primary excitation. Therefore, ELS data can be collected rapidly compared to VBXPS data. However, the primary electron-beam current must be kept low enough so that electron-beam damage to the surface is minimized.[25]

ELS has been used to study the optical properties of Ag and other metals.[49–52] The features in the loss spectrum of Ag are well documented, but the interpretation of their origin is still controversial. The reason for the uncertainty in the interpretation of the Ag loss spectra is mainly due to the difficulty in determining which physical process is responsible for a given loss feature during the inelastic scattering of electrons at the surface. These processes include creation of volume and surface plasmons and interband and interband transitions and possibly momentum transfer of scattered electrons as well as multiple scattering events. The analysis and interpretation of ELS data are complex. In order to assign features due to electronic transitions, it is necessary to have a good representation of the electronic band structure of the material under study. Moreover, plasmon features complicate interpretation of the ELS data of metals. Plasma oscillations in a metal are defined as the collective longitudinal excitation of the conduction-electron gas. Plasmons are quantized plasma, which can be excited by passing an electron beam through a metal film or reflecting electrons off the surface. The reflected or transmitted electron beam will typically exhibit energy losses equal to integral multiples of the plasmon loss energy. Depending on the electronic oscillations, plasmons are classified as surface (transverse) or volume (longitudinal). The energy loss from the surface and volume plasmons in the free-electron approximation is related by

$$E_{\mathrm{sp}}=\frac{E_{\mathrm{vp}}}{\sqrt{2}}. \tag{1}$$

The interpretation of ELS data is further complicated because multiple-loss features consisting of both surface and volume plasmons may be present in the spectra.

Seah[50] provides a general description of several methods that have been developed to assign the nature of the various features. One technique consists of varying the primary-beam energy in order to observe intensity changes in the spectral features. The probability of exciting a surface plasmon for a metal[53] is given by

$$P=(\pi e^2/2\hbar)[m/(2E_0)]^{1/2}, \tag{2}$$

where E_0 is the primary-beam energy, m the electron mass, and e the electron charge. Based on this equation, decreasing the primary-beam energy increases the probability of exciting surface-plasmon losses so the intensities of surface-plasmon features increase. Furthermore, the intensities of bulk plasmons decrease. This variation in surface and volume-plasmon intensities is demonstrated in an ELS study of Sn metal by Hoflund and Corallo[48] in which the surface sensitivity was varied by changing both the primary-beam energy and the incidence and collection angles in the experiment. The variations in the relative intensities of surface and bulk plasmons and the multiple-loss features follow the expected trends. If these trends are not followed, then the features are due to interband or intraband transitions, which have more complex intensity variations with primary-beam energy.

EXPERIMENT

Three samples were examined in this study including a Ag foil (99.99+% purity) from Goodfellow, a AgO powder (99% purity) from Aesar, and a Ag_2O powder (99+% purity) from Alfa. The Ag foil was cleaned by Ar^+ sputtering until no O or C contaminants could be observed using XPS. The AgO and Ag_2O powders were pressed into Al cups and inserted into the UHV system, where they were heated under vacuum at 130 °C for 30 min to reduce the surface contamination levels consisting of hydrocarbons, Ag carbonate/bicarbonate, water, and hydroxyl groups. The Ag oxides were not sputtered because this may alter the O-to-Ag atom ratio and induce structural damage.

After the various treatments the samples were characterized using XPS and ELS in a Perkin-Elmer PHI 5600 system. The XPS data (nonmonochromatized) were taken using an Al anode in the high-energy-resolution mode. The ELS data were taken using primary-electron-beam energies ranging from 100 to 2000 eV, and the primary-beam energy maximum was used to set the zero point of the spectra. The full width at half maximum (FWHM) of the primary-beam energy distribution was approximately 0.6 eV. The primary electron beam and the analyzer were each 45° off the sample normal.

RESULTS AND DISCUSSION

Ag^0 ELS

The electronic band structure of silver has been studied extensively using experimental as well as theoretical models.[53–60] These studies show that silver possesses interesting and unique characteristics among the transition and noble metals. Silver has relatively narrow $4d$ bands, which are located about 4 eV below the Fermi energy (E_F) level. For this reason its optical properties have characteristics of both free and bound electrons. The free-electron contribution arises from a strong hybridization of the s and p orbitals.

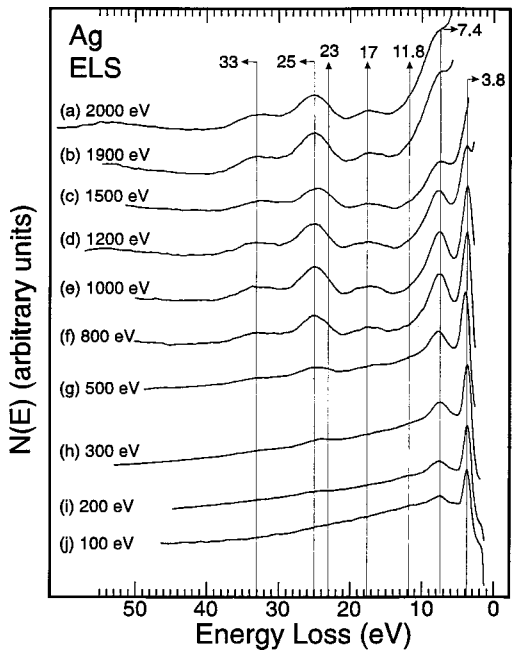

FIG. 1. Electron energy-loss spectra obtained from a cleaned polycrystalline Ag metal surface for primary energies of (a) 2000, (b) 1900, (c) 1500, (d) 1200, (e) 1000, (f) 800, (g) 500, (h) 300, (i) 200, and (j) 100 eV.

The loss spectra obtained from polycrystalline silver metal are shown in Figs. 1(a)–1(j) for energies ranging from 2000 to 100 eV, respectively. Two peaks at 3.8 and 7.4 eV dominate the low-energy spectra. Although the 3.8-eV feature has been attributed to various loss processes, Seah[50] has shown that it is due to a surface-plasmon loss. However, there is no feature at a loss energy of 5.35 eV that would correspond to a bulk-plasmon loss feature as predicted by Eq. (1). This may be due to the fact that Ag is not a free-electron-like metal. Otto and Petri[61] have suggested that the 7.4-eV feature is due to creation of volume plasmons. This is consistent with a study of the optical properties of Ag by Ehrenreich and Philipp,[59] who find that the energy-loss function peaks at 7.5 eV near the free-electron plasma frequency. The assignment of the 7.4-eV loss peak as a bulk-plasmon loss peak is consistent with the data shown in Fig. 1. As the primary-electron-beam energy is increased from 100 to 2000 eV, the 7.4-eV feature becomes more prominent compared to the 3.8-eV feature. This is the correct intensity variation if the former is due to a bulk-plasmon loss and the latter is due to a surface-plasmon loss. The probabilities of exciting surface plasmons for several primary-beam energies calculated using Eq. (2) are shown in Table I. Although not apparent from the data shown in Fig. 1 because the intensities of these spectra were scaled arbitrarily by the data collection software, the intensity of the 3.8-eV feature decreases as the primary-electron-beam energy increases. Ingram, Nebesny, and Pemberton[52] have performed ELS on polycrystalline Ag using primary-electron-beam energies of 200 and 1500 eV. They found that the peak-area ratio of the 3.8-eV feature and the elastic peak decreases from 0.08 to 0.02 as E_p increases from 200 to 1500 eV. Another argument for the 3.8-eV feature assignment as a surface-plasmon loss feature is that there are no interband transitions that might be responsible for this feature. The Ag $4d$ electrons lie in a band ranging from 4 to 7 eV below E_F so 3.8 eV is not enough energy to excite these electrons to unfilled levels. The *s-p* electrons lying closer to E_F have a low and broad intensity distribution and would not yield a sharp, well-defined feature like the 3.8-eV peak. Seah[49] has made an attempt to interpret the 3.8- and 7.8-eV features as due to interband transitions based on the calculated band structure of Ag and concluded that a reasonable explanation could not be given because the most intense transitions do not yield the experimentally observed loss energies. In this study Seah tentatively assigned this 3.8-eV loss feature as due to bulk-plasmon formation but later demonstrated that it is due to surface-plasmon formation.[50]

TABLE I. Probabilities of surface-plasmon excitations for Ag^0.

E_0 (eV)	Probability	E_0 (eV)	Probability
100	0.58	1000	0.18
200	0.41	1200	0.17
300	0.33	1500	0.15
500	0.26	1900	0.13
800	0.20	2000	0.13

Another feature is present in the 100- and 200-eV loss spectra centered at 1.8 eV, which has not been observed in previous Ag ELS studies. It could possibly be due either to a surface-plasmon loss or an interband transition. If it is a surface-plasmon loss feature, then Ag would have two surface-plasmon loss features, and this is unlikely. Furthermore, assigning the 1.8-eV feature as a surface-plasmon loss feature and the 3.8-eV feature as due to two surface-plasmon losses is not reasonable because multiple-loss features are always smaller than single-loss features. The other possibility is an assignment due to an interband transition. Arlinghaus, Gay, and Smith[62] have performed fully self-consistent electronic-structure calculations on the Ag(100) surface and found an unexpectedly high density of surface states. They suggest that these surface states are important in determining the physical and chemical properties of *d*-band metals. Reihl, Schlittler, and Neff[63] identified a Schockley-type surface state lying within the *s-p* hybridization gap at 1.7 eV above E_F at the $\bar{X}$ point of the surface Brillouin zone on Ag(110) using angle-resolved inverse photoemission spectroscopy. Based on these findings, the 1.8-eV loss feature in Fig. 1 is assigned as due to an interband transition loss from the top of the filled *s-p* band to the surface states lying just above E_F.

There is also a very small peak visible in the Ag loss spectra centered around 11.8 eV. This peak has been identified in a previous study by Seah,[49] who suggested that it may be assigned as a multiple loss feature consisting of the 3.8-eV and 7.4-eV loss features. If this were the case, then this feature should lie at 11.2 eV. Silver has been shown to have a characteristic interband transition around 11.9 eV due to the excitation of electrons from the $2s$ orbital to the $5p$ orbital and $4p$-$5d$ hybridized conduction band, and this is believed to be the origin of the 11.8-eV peak observed in this study.

The higher-energy ELS features become more prominent and well defined with increasing primary beam energy up to 2000 eV. The three most prominent features lie at 17, 25,

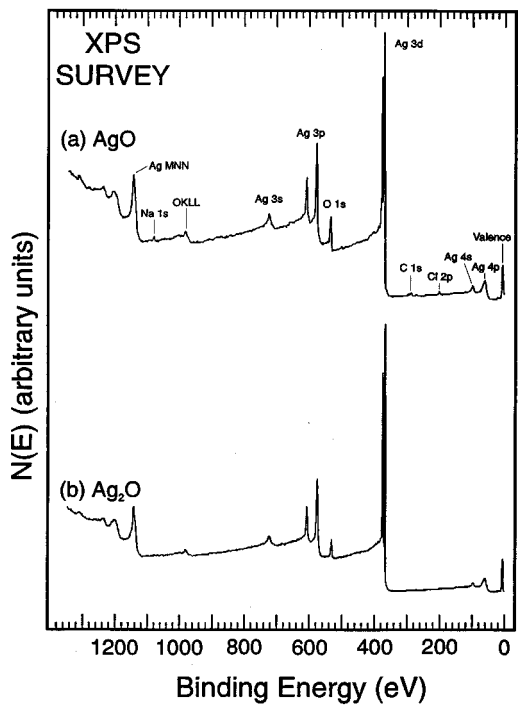

FIG. 2. XPS survey spectra obtained from (a) the AgO sample after a 130 °C anneal for 30 min and (b) the Ag_2O sample after a 300 °C anneal for 30 min.

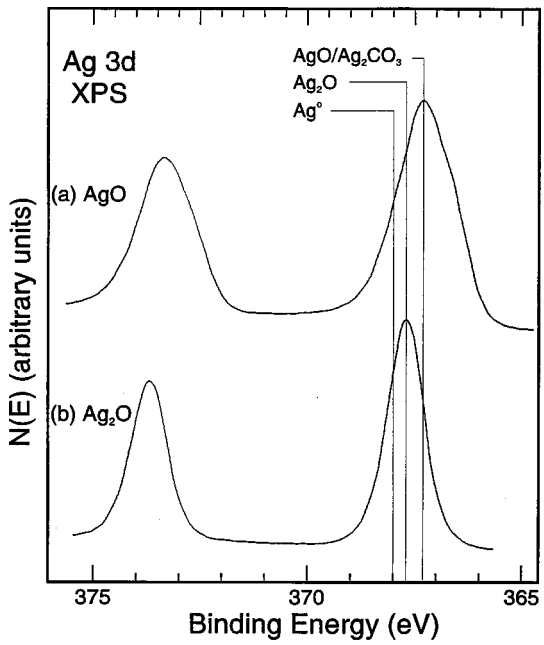

FIG. 3. High-resolution XPS Ag 3*d* spectra obtained from (a) the AgO sample after a 130 °C anneal for 30 min and (b) the Ag_2O sample after a 300 °C anneal for 30 min.

and 33 eV, and a smaller feature may be present as a shoulder at 23 eV. Since these features are not apparent at lower primary-beam energies, they may be due to volume plasmons or interband transitions that may not be allowed or have small cross sections in the potential field near the surface. A study by Wehner *et al.*[57] of the Ag valence structure indicates the presence of an interband transition near 17.5 eV. The intensity of this peak is very low and its shape and width were not resolved. Eckardt, Fritsche, and Noffke[55] have carried a self-consistent relativistic calculation of the band structure of Ag. Their results indicate that there are numerous positions in the Brilluoin zone that would yield loss energies similar to those of the higher-energy ELS features.

AgO XPS

The thermal decomposition of AgO has been studied by Weaver and Hoflund[1] using XPS. Results from this study show that AgO is stable in UHV at temperatures up to 100 °C. Annealing at this temperature for 30 min causes partial decomposition of surface contaminants such as hydrocarbons, carbonates, and others. The decomposition of AgO becomes significant at temperatures above 200 °C. In the present study XPS data were obtained from the as-entered AgO sample to determine the amount of surface contamination present. As expected, there was a considerable amount of hydrocarbons present in the near-surface region. The sample was annealed for 30 min at 100 and then 130 °C to reduce the amounts of contaminants. Higher temperatures were not used to avoid decomposition of the AgO. The XPS survey spectrum obtained from the 130 °C–annealed AgO sample is shown in Fig. 2(a). The peaks visible in this spectrum include the Ag core level and Auger peaks, the O 1*s* and Auger peaks, the valence-band peak, and small peaks due to contaminants including C, Na, and Cl. These contaminants are usually present on oxide surfaces, and a determination of the composition based on the homogeneous assumption indicates that each of these contaminants is present at the several percent level.

The high-resolution XPS Ag 3*d* peaks obtained from the AgO sample after the 130 °C anneal is shown in Fig. 3(a). The binding energy (BE) of the $3d_{5/2}$ peak is 367.3 eV, and its FWHM is 1.57 eV. These values are in good agreement with previously published XPS data for AgO.[1,7,8,27] As discussed by Weaver and Hoflund,[1] the relatively high FWHM of the Ag $3d_{5/2}$ peak is attributed to the presence of both Ag^+ and Ag^{3+} ions in the crystal lattice of AgO. Park *et al.*[64] have calculated the electronic structure for AgO and conclude that the two Ag ions are Ag^+ and Ag^{2+} due to the presence of holes on the oxygen species. The fact that the Ag 3*d* peaks obtained from AgO are so broad supports the assertion that two Ag valencies are present. However, both possible explanation contain aspects that seem unrealistic. In the former it is difficult to understand how Ag^{3+} forms particularly when other Ag compounds of this valency have not been found. However, Au, which is just below Ag in the periodic table, does form Au^{3+} ions in Au_2O_3. In the latter, $O^{-1.5}$ species would be present, and these also have not been observed previously. Further effort will be required to resolve this issue.

The O 1*s* spectrum obtained from the AgO sample after annealing at 130 °C for 30 min is shown in Fig. 4(a). The shape indicates that multiple chemical states of oxygen are present. The predominant O feature due to AgO has a BE of 528.4 eV. The BE assignment of this peak has been discussed in detail by Weaver and Hoflund[1] and is in good agreement with previously published data.[1,62] The other large

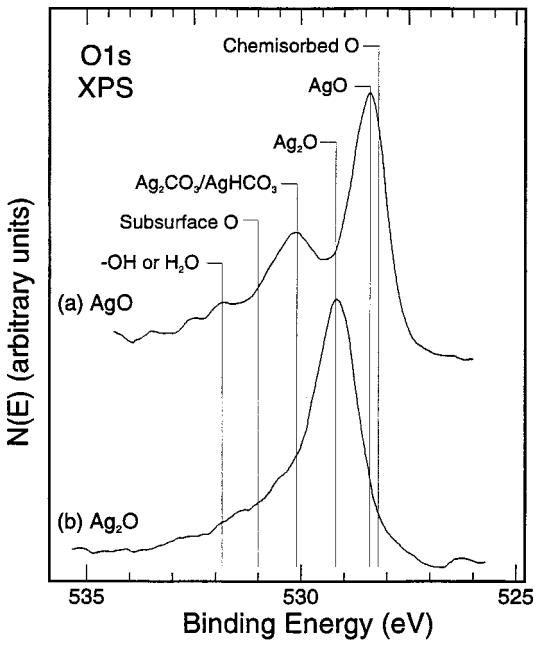

FIG. 4. High-resolution XPS O 1*s* spectra obtained from (a) the AgO sample after a 130 °C anneal for 30 min and (b) the Ag_2O sample after a 300 °C anneal for 30 min.

peak present in the O 1*s* spectrum is due to Ag carbonate or bicarbonate at a BE of 530.1.[8,20,26] These species most likely form by adsorption of CO_2 during air exposure. The broad shoulder visible in the O 1*s* spectrum at binding energies between 531 and 532 eV are due to contributions from hydroxyl groups and adsorbed water.

The C 1*s* spectrum obtained from the 130 °C annealed AgO sample is shown in Fig. 5. The peak with a BE of about 284 is due to adsorbed hydrocarbons. The peak centered at 287.6 eV is attributed to the presence of silver carbonate and

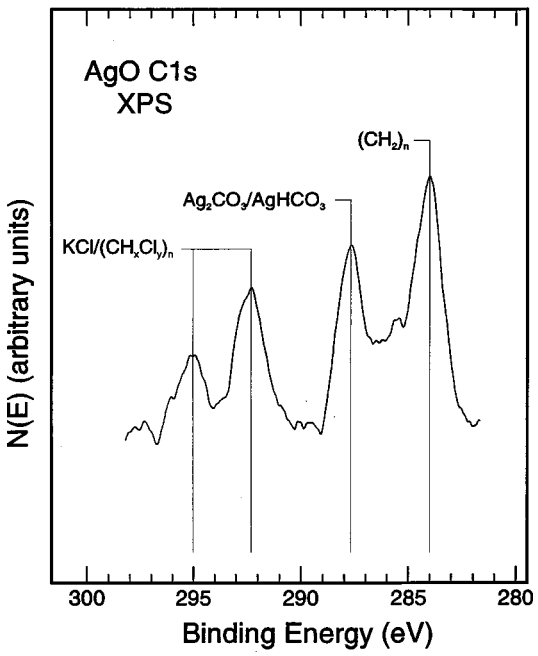

FIG. 5. High-resolution XPS C 1*s* spectrum obtained from the AgO sample after a 130 °C anneal for 30 min.

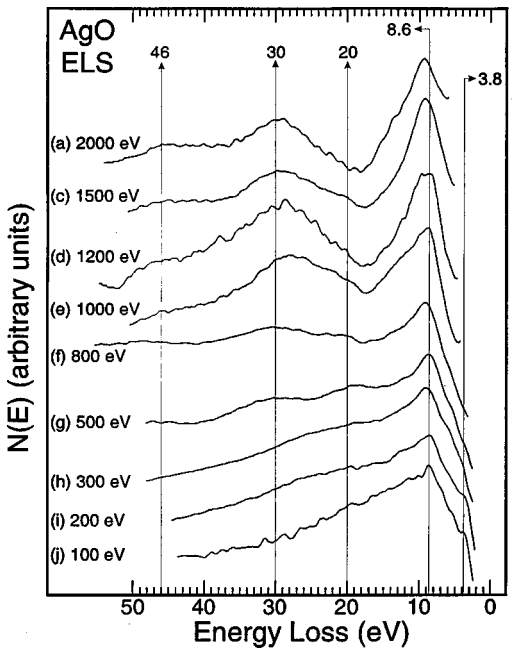

FIG. 6. Electron energy-loss spectra obtained from the AgO sample after annealing at 130 °C for 30 min using primary beam energies of (a) 2000, (b) 1500, (c) 1200, (d) 1000, (e) 800, (f) 500, (g) 300, (h) 200, and (i) 100 eV.

bicarbonate, which is consistent with the O 1*s* spectrum. The previous study of the thermal decomposition of AgO also found[1] that carbonate species and hydrocarbons are present as the two major contaminants in AgO. There are two other peaks present in this spectrum centered at BE's of 292.3 and 295.0 eV. These peaks are due to a potassium chloride or Cl-containing contaminant species. The amounts of these contaminant species are very small and therefore would have a small influence on the ELS spectra as discussed below.

AgO ELS

The electron energy loss spectra obtained from the 130 °C–annealed AgO sample is shown in Figs. 6(a)–6(j) for primary-beam energies ranging from 2000 to 100 eV, respectively. By increasing the primary-beam energy, deeper layers of the AgO sample are probed due to an increase in the inelastic mean free path of the electrons with kinetic energy. These spectra are clearly different from those obtained from Ag metal. An intense peak centered at a loss energy of 8.6 eV dominates the lower-energy spectra. The intensity of this peak increases with increasing primary energy beam, and it predominates throughout the whole range of primary-beam energies used. A shoulder is also present at a loss energy of about 10 eV. This feature is most apparent at primary beam energies of 1000 and 1200 eV. It is absent in the lower-energy spectra and becomes the predominant feature in the higher energy spectra, shifting the feature from 8.6 toward 10 eV loss energy.

In addition to the main feature, there are several shoulders centered at loss energies of 6.8, 5.4, and 3.8 eV. Due to their low intensities, the presence of these shoulders is most likely due to contributions from chemical species located close to the surface region and in low concentrations. A study by Barteau and Madix[65] found that filled energy levels due to

adsorbed surface carbonates on silver, observed using XPS, are located at energies of 2.0, 3.5, 8.4, and 10.4 eV below E_F. Therefore, the presence of surface carbonates and other impurities may contribute to the formation of these loss features and possibly the shift of the 8.6-eV feature.

The spectra obtained using higher primary-beam energies are characterized by the appearance of a broad peak centered around 30 eV. The intensity of this peak increases with increasing primary-beam energy. In addition to this main feature, there are two smaller loss features centered at 20 and 46 eV. These peaks are apparent in the 800-eV primary-beam loss spectra. Since AgO is a semiconductor, the loss features are most likely due to interband transitions. The physical processes that form these loss features cannot be specified because the electronic structure of AgO has not been published. Although this is a disadvantage with regard to interpreting AgO ELS data at this time, a comparison of the ELS data obtained from Ag metal and various Ag compounds such as AgO and Ag_2O is quite useful to gain a better understanding of the differences between these two oxides. Furthermore, the ELS spectra presented in this paper have recently been used to determine the chemical state of Ag in alumina-supported Ag ethylene epoxidation catalysts.[66] This has not been possible using other techniques.

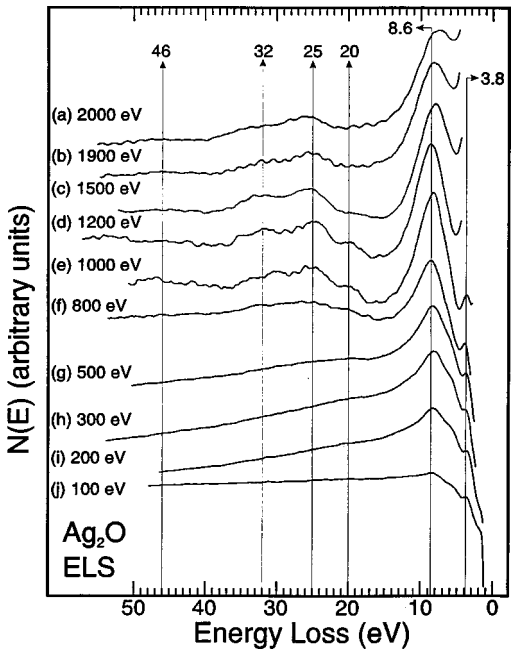

FIG. 7. Electron energy-loss spectra obtained from the Ag_2O sample after annealing at 300 °C for 30 min using primary energies of (a) 2000, (b) 1900, (c) 1500, (d) 1200, (e) 1000, (f) 800, (g) 500, (h) 300, (i) 200, and (j) 100 eV.

Ag_2O XPS

Weaver and Hoflund[2] have studied the thermal decomposition of Ag_2O using XPS. Their results showed that annealing at 100 °C reduces the amounts of contaminants such as carbonates and hydrocarbons. At this temperature they recorded a slight increase in the concentration of AgO due to a disproportionation reaction that occurs at the surface of Ag_2O. Annealing at 200 °C causes the decomposition of surface carbonate contaminants and a partial reduction of the AgO back to Ag_2O. After a 300 °C anneal all of the AgO present is transformed into Ag_2O and most of the impurities are eliminated. A small amount of metallic silver also forms through decomposition of Ag_2O. After annealing at 490 °C, most of the Ag_2O decomposes to Ag metal. A migration of impurities from the bulk to the surface occurs as well. In this present study an annealing temperature for Ag_2O of 300 °C was chosen since complete decomposition of the contaminants is achieved while the thermal decomposition Ag_2O is negligible.

Based on these results the Ag_2O sample was analyzed using XPS before and after a 300 °C anneal for 30 min. The XPS survey spectrum obtained from Ag_2O after annealing is shown in Fig. 2(b). The results obtained are very similar to those described above for AgO. The peaks visible in this spectrum include the Ag core level and Auger peaks, the O 1*s*, and Auger peaks and the valence-band peaks. No C 1*s* peak is apparent. The concentrations of Ag and O calculated using the area under the Ag $3d_{5/2}$ and O 1*s* peaks, published sensitivity factors and the homogeneous assumption indicate that the near-surface region is composed of 30% O and 70% Ag, which is within the experimental error for Ag_2O.

The high-resolution Ag 3*d* spectrum is shown in Fig. 3(b). The Ag $3d_{5/2}$ peak has a BE of 367.7 eV and a FWHM of 1.0 eV. This FWHM is much lower than that of AgO due to the facts that the Ag_2O surface contains fewer contaminants and most importantly because Ag_2O contains only Ag^{1+} species, while AgO contains an equimolar mixture of Ag^{1+} and Ag^{3+} to give an average valency of Ag^{2+}.

The O 1*s* spectrum obtained from the Ag_2O sample after a 300 °C anneal is shown in Fig. 4(b). The O 1*s* peak due to oxygen from Ag_2O has a BE of 529.2 eV, and there is a shoulder present at the high-BE side of the O 1*s* peak that extends from 530 eV up to 532.5 eV, indicating the presence of oxygen in other chemical states including silver carbonate and bicarbonate, adsorbed water, and possibly an oxygen-containing *C* species. These species, if present, are found in very small quantities.

Ag_2O ELS

The ELS spectra obtained from the Ag_2O sample after a 300 °C anneal for 30 min are shown in Figs. 7(a)–7(j) for primary energies ranging from 2000 to 100 eV respectively. The main feature in all of these spectra is centered around 8.6 eV, and its intensity increases with increasing primary beam energy from 100 to 1000 eV and then apparently remains constant to 2000 eV. A comparison of this peak with the 8.6-eV feature present in the loss spectra of AgO provide an indication of the similarities in the electronic excitation levels of these two oxides. The 8.6-eV peak from Ag_2O differs from the corresponding AgO feature in that as the primary beam energy is increased the Ag_2O peak gradually broadens to lower loss energies centered around 8.2 eV while the AgO peak broadens to higher loss energies around 9.4 eV.

The electronic structure of Ag_2O has been investigated previously by Tjeng *et al.*[67] using photoelectron, Auger-electron and bremsstralung isochromat spectroscopy. The band gap for Ag_2O was calculated to be 1.3 eV with the

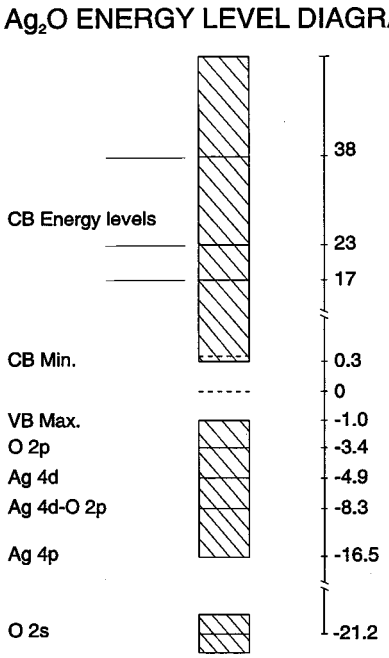

FIG. 8. Energy-level diagram for Ag_2O.

bottom of the conduction band located at 0.3 eV and the top of the valence band at -1.0 eV with respect to E_F. This same study also shows that the Ag $4d$ and O $2p$ orbitals mix to give a hybrid band structure that is 8.3 eV below E_F. The 8.6-eV peak present in the loss spectrum of Ag_2O is likely to be due to a interband transition from the Ag $4p-$O $2p$ valence band to the bottom of the conduction band (-8.3 eV$\rightarrow$0.3 eV), resulting in a 8.6 eV loss feature. A graphical representation of the electronic band structure of Ag_2O obtained from previous studies[62,67] is shown in Fig. 8. Conduction band gaps are estimated from the ELS data obtained from Ag_2O in this study.

The other feature visible in the lower primary beam energy spectra is centered at 3.8 eV. This peak gains intensity as the primary beam energy is increased and is visible up to primary energies of 1000 eV, and then it becomes incorporated into the broadening elastic peak. The origin of the 3.8-eV peak probably is due to an interband transition from the O $2p$ band located 3.4 eV below E_F to the conduction-band minimum (-3.4 eV$\rightarrow$0.3 eV), resulting in a loss of 3.7 eV. The 3.8-eV feature is also present in the AgO spectra, but its intensity is much weaker. This could result from partial reduction of AgO during the 130 °C anneal forming some Ag_2O. In addition to the 3.8- and 8.6-eV features in the Ag_2O spectra, there are two shoulders visible around 1.5 and 5.4 eV. These features are consistent with interband transitions from the valence-band maximum (-1.0 eV$\rightarrow$0.3 eV) and Ag $4d$ bands (-4.9 eV$\rightarrow$0.3 eV) to the conduction-band minimum state, respectively.

The higher beam primary energy spectra are characterized by a broad feature containing loss contributions centered around 20, 25, and 32 eV. The physical or optical phenomena responsible for the excitation of these peaks is not easily understood due to a lack of knowledge of the energy levels of empty conduction bands in Ag_2O. The 20-eV feature can be attributed to a core-to-valence-band transition from the O $2s$ band located 21.2 eV below E_F. The 25-, 32-, and 46-eV features are probably due to contributions from interband transitions from the valence or O $2s$ levels to unfilled levels. The positions of the expected energy levels of conduction bands are shown in Fig. 8 as a result of the analysis of the Ag_2O loss spectra obtained in this study. Electronic structure calculations are needed in order to determine the positions and contributions of these conduction bands more accurately.

CONCLUSIONS

The electron energy-loss spectra for silver metal and its two oxides AgO and Ag_2O have been obtained and analyzed in this study. The three sets of ELS spectra are quite different as expected. Therefore, ELS is a useful technique for distinguishing between Ag metal, AgO, and Ag_2O. Since silver is a conductor, its electronic structure favors plasmon excitation contributions to its loss spectra. Silver oxides are semiconductors with relatively wide band gaps, which favors interband transition from core and valence-band electrons to unfilled energy levels. XPS was used in conjunction with ELS in order to characterize the chemical states and amounts of contaminants present at these oxide surfaces. The analysis of the loss spectra from AgO and Ag_2O is not straightforward, and a detailed understanding of the contributions to these spectra must be based on both filled and empty electronic levels, which have not yet been determined for these oxides.

[1] J. F. Weaver and G. B. Hoflund, J. Phys. Chem. **98**, 8519 (1994).
[2] J. F. Weaver and G. B. Hoflund, Chem. Mater. **6**, 1693 (1994).
[3] G. B. Hoflund, J. F. Weaver, and W. S. Epling, Surf. Sci. Spectra **3**, 157 (1994).
[4] G. B. Hoflund, J. F. Weaver, and W. S. Epling, Surf. Sci. Spectra **3**, 163 (1994).
[5] G. B. Hoflund, J. F. Weaver, and W. S. Epling, Surf. Sci. Spectra **3**, 151 (1994).
[6] G. R. Corallo, G. B. Hoflund, and R. A. Outlaw, Surf. Interface Anal. **12**, 185 (1988).
[7] G. Schön, Acta Chem. Scand. **27**, 2623 (1973).
[8] J. S. Hammond, S. W. Gaarenstroom, and N. Winograd, Anal. Chem. **47**, 2193 (1975).
[9] F. Yubero, J. M. Sanz, E. Elizande, and L. Galán, Surf. Sci. **251**, 296 (1991).
[10] R. P. Nielsen and J. H. LaRochelle, U.S. Patent No. 3,962,136 (1976) and U.S. Patent No. 4,012,426 (1977).
[11] J. M. Berty, in *Applied Industrial Catalysis*, edited by B. E. Leach (Academic, New York, 1983–1984), Vol. 1, p. 207.
[12] C. N. Satterfield, *Heterogeneous Catalysis in Industrial Practice*, 2nd ed. (McGraw-Hill, New York, 1991).
[13] R. A. van Santen and H. P. Kuipers, Adv. Catal. **35**, 265 (1987).
[14] D. M. Minahan and G. B. Hoflund, J. Catal. **158**, 109 (1996).
[15] G. B. Hoflund and D. M. Minahan, J. Catal. **162**, 48 (1996).
[16] D. M. Minahan, G. B. Hoflund, W. S. Epling, and D. W. Schoenfeld, J. Catal. **168**, 393 (1997).

[17] W. S. Epling, G. B. Hoflund, and D. M. Minahan, J. Catal. **171**, 490 (1997).
[18] G. B. Hoflund and D. M. Minahan, Nucl. Instrum. Methods Phys. Res. B **118**, 517 (1996).
[19] Y. Yung, D. Jingfa, Y. Xiaohong, and Z. Shi, Appl. Catal., A **92**, 73 (1992).
[20] A. I. Boronin, V. I. Bukhtiyarov, A. L. Vishneskii, G. K. Boreskov, and V. I. Sachenko, Surf. Sci. **201**, 195 (1988).
[21] S. N. Gorcharova, E. A. Paukshtis, and B. S. Bal'zhinimaev, Appl. Catal., A **126**, 67 (1995).
[22] R. A. Outlaw, S. N. Sankaran, G. B. Hoflund, and M. R. Davidson, J. Mater. Res. **3**, 1378 (1988).
[23] R. A. Outlaw, D. Wu, M. R. Davidson, and G. B. Hoflund, J. Vac. Sci. Technol. A **6**, 70 (1988).
[24] G. B. Hoflund and J. F. Weaver, Meas. Sci. Technol. **5**, 201 (1994).
[25] G. B. Hoflund, Scanning Electron Microsc. IV, 1391 (1995).
[26] C. Rehren, M. Muhler, X. Bao, R. Schlögl, and G. Ertl, Phys. Z. Chem. **174**, 11 (1991).
[27] S. W. Gaarenstroom and N. J. Winograd, Chem. Phys. **67**, 15 (1977).
[28] V. K. Kaushik, J. Electron Spectrosc. Relat. Phenom. **56**, 273 (1991).
[29] M. Romand, M. Roubin, and J. P. Delourne, J. Electron Spectrosc. Relat. Phenom. **13**, 229 (1978).
[30] R. Holm and S. Storp, J. Electron Spectrosc. Relat. Phenom. **8**, 459 (1976).
[31] S. Evans, E. L. Evans, D. E. Parry, M. J. Tricker, M. J. Walters, and J. M. Thomas, Faraday Discuss. Chem. Soc. **58**, 97 (1975).
[32] W. S. Epling, G. B. Hoflund, and G. N. Salaita, J. Phys. Chem. B **102**, 2263 (1998).
[33] G. N. Salaita, Z. F. Hazos, and G. B. Hoflund, J. Electron Spectrosc. Relat. Phenom. **107**, 73 (2000).
[34] E. Paparazzo, G. Fierro, G. M. Ingo, and N. Zacchetti, Surf. Interface Anal. **12**, 438 (1988).
[35] W. S. Epling, C. K. Mount, and G. B. Hoflund, Appl. Surf. Sci. **134**, 187 (1998).
[36] M. A. Stranick and A. Moskwa, Surf. Sci. Spectra **2**, 45 (1993).
[37] M. A. Stranick and A. Moskwa, Surf. Sci. Spectra **2**, 50 (1993).
[38] R. A. Powell, Appl. Surf. Sci. **2**, 397 (1979).
[39] C. L. Lau and G. K. Wetheim, J. Vac. Sci. Technol. **15**, 622 (1978).
[40] D. F. Cox and G. B. Hoflund, Surf. Sci. **151**, 202 (1985).
[41] J.-M. Themlin, M. Chtaib, L. Henrard, P. Lambin, J. Darville, and J.-M. Gilles, Phys. Rev. B **46**, 2460 (1992).
[42] P. M. A. Sherwood, Phys. Rev. B **41**, 10 151 (1990).
[43] J.-M. Themlin, R. Sporken, J. Darville, R. Caudano, J.-M. Gilles, and R. L. Johnson, Phys. Rev. B **42**, 11 914 (1990).
[44] G. B. Hoflund and G. R. Corallo, Phys. Rev. B **46**, 7110 (1992).
[45] G. B. Hoflund, Chem. Mater. **6**, 562 (1994).
[46] F. Gauzzi, B. Vedini, A. Maddalena, and G. Principi, Inorg. Chim. Acta **104**, 1 (1985).
[47] F. Gauzzi and B. Vedini, J. Mater. Sci. Lett. **4**, 1492 (1985).
[48] G. B. Hoflund and G. R. Corallo, Surf. Interface Anal. **13**, 33 (1988).
[49] M. P. Seah, Surf. Sci. **17**, 161 (1969).
[50] M. P. Seah, Surf. Sci. **24**, 357 (1971).
[51] J. C. Ingram, K. W. Nebesny, and J. E. Pemberton, Appl. Surf. Sci. **44**, 279 (1990).
[52] J. C. Ingram, K. W. Nebesny, and J. E. Pemberton, Appl. Surf. Sci. **44**, 293 (1990).
[53] E. A. Stern and R. A. Ferrell, Phys. Rev. **120**, 130 (1960).
[54] O. Jepsen, D. Glötzel, and A. R. Mackintosh, Phys. Rev. B **23**, 2684 (1981).
[55] H. Eckardt, L. Fritsche, and J. Noffke, J. Phys. F **14**, 97 (1984).
[56] T. K. Sham, Phys. Rev. B **31**, 1888 (1985).
[57] P. S. Wehner, R. S. Williams, S. D. Kevan, D. Denlev, and D. A. Shirley, Phys. Rev. B **19**, 6164 (1979).
[58] R. Courths, H. Wern, U. Hau, B. Cord, V. Bachelier, and S. Hüfner, J. Phys. F **14**, 559 (1984).
[59] H. Ehrenreich and H. R. Philipp, Phys. Rev. **128**, 1622 (1962).
[60] G. Leveque, C. G. Olson, and D. W. Lynch, Phys. Rev. B **27**, 4654 (1983).
[61] A. Otto and E. Petri, Solid State Commun. **20**, 823 (1976).
[62] F. J. Arlinghaus, J. G. Gay, and J. R. Smith, Phys. Rev. B **23**, 5152 (1981).
[63] B. Reihl, R. R. Schlittler, and H. Neff, Surf. Sci. **152/153**, 231 (1985).
[64] K.-J. Park, D. I. Novikov, V. A. Gubanov, and A. J. Freeman, Phys. Rev. B **49**, 4425 (1994).
[65] M. A. Barteau and R. J. Madix, J. Electron Spectrosc. Relat. Phenom. **31**, 101 (1983).
[66] G. B. Hoflund, J. F. Weaver, G. N. Salaita, and D. M. Minahan, *Catalyst Deactivation* (Elsevier, New York, 1999).
[67] L. H. Tjeng, M. B. J. Meinders, J. van Elp, J. Ghijsen, G. A. Savatsky, and R. L. Johnson, Phys. Rev. B **41**, 3190 (1990).